Molecular Crystals and Liquid Crystals
Publication details, including instructions for authors and subscription information:
http://www.tandfonline.com/loi/gmcl20

Study on Dispersion of Liquid Crystal Droplets in PDCLC Film by 2D/3D-FTIR Spectrum

J. H. Wang [a], B. Y. Zhang [a], M. Xi [a] & X. Y. Xu [a]
[a] The Science College of Shenyang University, Shenyang, China

Version of record first published: 07 Oct 2011

To cite this article: J. H. Wang, B. Y. Zhang, M. Xi & X. Y. Xu (2011): Study on Dispersion of Liquid Crystal Droplets in PDCLC Film by 2D/3D-FTIR Spectrum, Molecular Crystals and Liquid Crystals, 548:1, 17-27

To link to this article: http://dx.doi.org/10.1080/15421406.2011.590341

Mol. Cryst. Liq. Cryst., Vol. 548: pp. 17–27, 2011

ISSN: 1542-1406 print/1563-5287 online
DOI: 10.1080/15421406.2011.590341

Taylor & Francis
Taylor & Francis Group

Study on Dispersion of Liquid Crystal Droplets in PDCLC Film by 2D/3D-FTIR Spectrum

J. H. WANG,* B. Y. ZHANG, M. XI, AND X. Y. XU

The Science College of Shenyang University, Shenyang, China

A polymer-dispersed chiral liquid crystal (PDCLC) film was fabricated by rapid polymerization of a trifunctional pre-polymer. The effect of applied voltage on optical rotation and transmittance of the PDCLC film was measured by a polarimeter (PerkinElmer Model 341) and was explained by the free-energy minimization process. The dispersion and size of liquid crystal (LC) droplets were observed by polarizing optical microscopy (POM) and Fourier transform infrared (FTIR) spectrometer with spectrum spotlight FTIR imaging system. The dispersion of LC droplets was depicted by the characteristic absorption peak of the $-C\equiv N$ group, which represents the LC droplets. The intensity of absorption by the $-C\equiv N$ group was shown by the peak height in the three-dimensional FTIR (3D-FTIR) spectrum. The size of LC droplets was assessed through an enlarged two-dimensional single-wavenumber FTIR (2D-FTIR) spectrum, and was found to be consistent with the results obtained by POM.

Keywords 3D/2D-FTIR; characteristic absorption peak; liquid crystals droplets; polymer-dispersed chiral liquid crystal

1. Introduction

Polymer-dispersed liquid crystal (PDLC) films, which consist of micron-sized droplets of liquid crystal (LC) and a polymer matrix, are specialized material for electro-optical devices [1–12]. The principle of operational PDLC films is based on light scattering from nematic LC micro-droplets under a controlled electric field. PDLC films have considerable potential use for large-area LC display devices and light control applications. Since these composite systems exhibit anisotropic optical and dielectric properties of nematic LCs, by choosing appropriate combinations of LCs and polymer materials, they can be optically switched from a highly light scattering state (OFF state) to a transparent state (ON state) due to mismatching and matching of the refractive indices of the polymer and the oriented LC droplets by applying an external electric field (thermal gradient or relatively small electrical voltage) [4,13–17]. In the OFF state, surface anchoring causes a non-uniform director field within the droplets, and the film scatters light due to the mismatching between the effective refractive index, n_{eff}, of LC droplets and the refractive index, n_{p}, of the polymer [18]. In the ON state, the director field is aligned along the applied electric field direction ($n_{\text{eff}} = n_{\text{p}}$), and for normal light incidence, the film becomes transparent if the ordinary refractive index n_{o} of LC droplets is equal to n_{p} [7,19,20]. The threshold voltage, V_{th}, and the response times τ_{R} and τ_{D} (rise and decay times, respectively), at which the PDLC switches from

*Address correspondence to J. H. Wang, The Science College of Shenyang University, Shenyang 110004, China. Tel.: +86-24-62266138. E-mail: jhwang1228@163.com

whiteness to transparency, and the optical contrast between the white and the transparent states are controlled by the size, shape [21,22], and anchoring energy of the LC domains. It is well established that the morphology of the LC droplets strongly affects the electro-optical properties of PDLC materials [23–28]. In general, the morphology is controlled by relative rates of phase separation, which depend on a number of factors, such as type of LC and pre-polymer, LC concentration, compatibility between the LC and the pre-polymer, and others. PDLCs films have a number of advantages over conventional low-molecular-mass LC displays. Some of the advantages are simple manufacturing, minimal fabrication cost, flexibility, a higher contrast ratio, and fast response time.

In the present research, we focused on the preparation of a PDCLC film and the analysis of the electro-optical behavior and morphologies of chiral liquid crystal (CLC) droplets in a polymer matrix. Such PDCLC systems could be used for preparing meso-/nano-sized multifunctional optical materials.

2. Experimental

2.1. Materials

Our composites of the PDCLC film were a solution of the monomer trimethylolpropane triacrylate (TMPTA, i.e., pre-polymer) and the photoinitiator 1173, which were supplied by Tianjin Tianjiao Chemical Company, China, and the CLC, which was a mixture of the chiral agent S-811 with the nematic LC 76G9700, which were supplied by Shijiazhuang Slichem Material Company, China. TMPTA is a transparent liquid, and its coefficient of refractive index is 1.4723. Nematic LC 76G9700 is a eutectic mixture of cyanobiphenyl and cyanoterphenyl ($n_o = 1.49$, $\Delta n = 0.15$, $T_{N\text{-}I} = 122^\circ$C). The mixture was achieved by stirring the components for several hours at a temperature above the phase transition temperature (T_{N-1}) of the CLC (the clearing point of the mixture of S-811 and 76G9700 is $T_{N-1} = 103.6^\circ$C). The structures of TMPTA, 1173, and S-811 are shown in Fig. 1.

2.2. Preparation of the PDLC Films

The mixture was injected between two indium–tin oxide (ITO)-coated glass plates at about 80°C and then cooled to room temperature (see Table 1 for the mixture's composition). The space between the two ITO-coated glass plates was determined to be 10 μm and was filled by aluminum foil. The mixture of CLC and pre-polymer (TMPTA) was injected into the space and then the aluminum foil was drawn out. The mixture was kept at a distance of 1 m from an ultraviolet (UV) light (1 kW) source and was exposed to UV for 3 min. Polymerization of the TMPTA occurred due to irradiation with UV light. Phase separation took place, with an increase in the TMPTA chain length, and micron-sized CLC droplets were separated from the polymer matrix.

Table 1. Composition of PDLC mixture with different component ratios

	76G9700	S-811	TMPTA	1173
Mixture	45%	0.3%	46%	8.7%

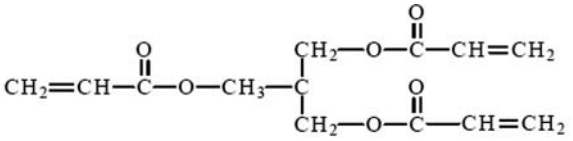

Trimethylolpropane Triacrylate (TMPTA)

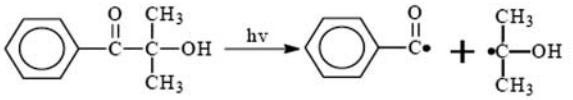

Photoinitiator 1173

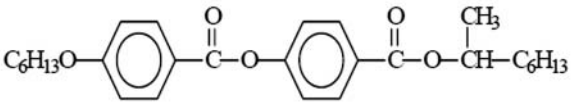

Chiral agent S-811 is a left-handed helical structure and white powder

Figure 1. Structure and properties of monomer TMPTA, photoinitiator 1173, chiral agent S-811, and nematic liquid crystal.

2.3. 2D/3D-FTIR

An infrared (IR) spectrum can characterize the different groups' absorption in complex molecules. A group's absorbable energy can be calculated as follows [29–34]:

$$E = h\upsilon, \tag{1}$$

where υ and h are vibration frequency and Planck's constant, respectively.

Energy is absorbed when a group's vibration frequency is equal to the infrared frequency. Thus, we can differentiate the groups according to their absorption frequencies. Although we can identify a group, we cannot describe its distribution in a sample by IR spectrum. A 2D/3D-FTIR (two/three-dimensional Fourier transform infrared) spectrum was used to describe the distribution of a group in the sample. For dual or multi-blending, we can describe the distribution of a special group which represents the molecule to determine the molecule's distribution in a blended system by the 2D/3D-FTIR spectrum. Of course, the special group is different from the others. The absorption peak of the $-C\equiv N$ group was chosen to characterize LC droplets. By assessing the dispersion of the $-C\equiv N$ group, we could assess the dispersion of CLC droplets. The absorbable wavenumber of the $-C\equiv N$ group was set at 2238 cm^{-1}.

2.4. Electro-Optical Properties Measurements

The electro-optical characteristics of the PDCLC film were measured by an experimental setup schematically shown in Fig. 2. A collimated beam of polarized Na light (wavelength 598 nm) was used as the incident light source. The optical rotation and transmittance of the PDCLC film were measured at a wavelength of 598 nm by a polarimeter (PerkinElmer Model 341). The curves for optical rotation and transmittance were described with regard to the change in electric voltage applied to the PDCLC film (Fig. 3).

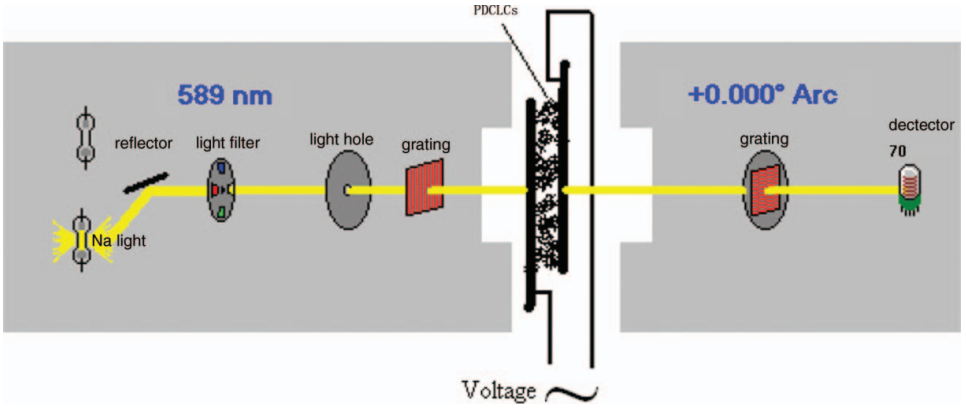

Figure 2. Schematic of the experimental setup.

2.5. Observation of the Morphology of the PDCLC Film

The size and dispersion of LC droplets are important factors that influence the optical properties of PDLC films. The monomer TMPTA has three acrylic functional groups in its backbone, which are responsible for the fast polymerization kinetics. Thus, by optimizing the number of these groups, we can obtain micron-sized CLC droplets by rapid polymerization. Polarizing optical microscopy (POM) was used for observing the morphology of the PDCLC film, and a 2D/3D-FTIR spectrum was firstly used for describing the dispersion and assessing the size of LC droplets in the PDCLC film.

3. Results and Discussion

3.1. Optical Properties of PDCLC Film

The effect of applied voltage on the optical rotation of the PDCLC film increased with the increase in voltage, as shown in Fig. 3(a). The optical rotation of the PDCLC film was

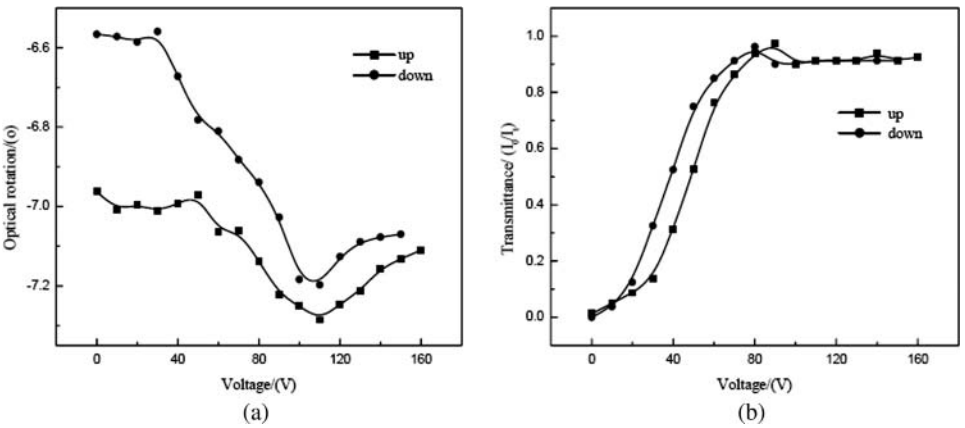

Figure 3. Effect of applied voltage on optical rotation and transmittance of PDCLC film: (a) optical rotation, (b) transmittance.

determined by the pitch of the CLC droplets, which in turn was affected by the voltage. The realignment or alignment of a CLC in an applied electric field, in a purely dielectric interaction, results from the system's tendency to minimize its total free energy [35]. This process can be described as the free-energy minimization process. The total free energy of the system is given by:

$$F_{\text{total}}=\frac{1}{2}\int dz\left[K_2\left(\frac{\partial\phi}{\partial Z}-q_0\right)^2-\Delta\varepsilon E^2\sin^2\phi\right], \tag{2}$$

where K_2 is the elastic constant, $q_0 = 2\pi/p_0$, E is the applied electric field, and $\Delta\varepsilon$ is the anisotropies in the dielectric constant, i.e., $\Delta\varepsilon = \varepsilon_{\parallel} - \varepsilon_{\perp}$. Generally, the total free energy minimizes with the increase in the applied voltage. The influence of voltage on the CLC is that the director field axis tends to align parallel to the electric field for positive dielectric anisotropies, and abnormal to the field for negative dielectric anisotropies. For cholesteric LC droplets, the realignment of the director field axis in the direction of the applied field will naturally affect the helical structure of the CLC. For $E < E_{\text{th}}$ (E_{th} is threshold electric field applied to the PDCLC film), the variation in pitch (P) with change in electric field is well approximated by the following expressions [35]:

$$P = P_0\left[1+\frac{(\Delta\varepsilon)^2P_0^4E^4}{32(2\pi)^4K_2^2}+\dots\right]. \tag{3}$$

It should be noted that the preceding treatment of field-induced changes in the pitch assumes that the cholesteric LC cell is thick and in an initially ideally twisted arrangement, and there is negligible influence of the cell walls. The pitch of cholesteric LC droplets depends on the average orientation of CLC director fields, which is determined by the balance between electric and elastic torques. As shown in Equation (3), the pitch of cholesteric LC droplets is lengthened with the increase in the applied voltage.

The rotatory power (in radians per unit length) is calculated as follows [36]:

$$\rho = -\pi(\delta n)^2\frac{P}{4\lambda^2} \tag{4}$$

The equation is satisfied when $\frac{1}{2}P\delta n \ll \lambda$, i.e., when the pitch is not too large $\Delta\varepsilon = \varepsilon_{\parallel} - \varepsilon_{\perp}$. The negative sign indicates that the direction of the rotation is opposite than that of the helical twist of the structure. As shown in Equation (4), the rotatory power is proportional to the pitch of cholesteric LC droplets. The optical rotation is induced by the rotatory power. As shown in Fig. 3(a), the optical rotation tends to be greater when the voltage is increased. Thus, the pitch of cholesteric LC droplets is lengthened by an increase in the applied voltage. The longest pitch and the maximum optical rotation are observed at 110 V. The optical rotation decreases when the applied voltage is sequentially increased further. The reason is that the change in the pitch of cholesteric LC droplets is determined by the competing electric and elastic forces. The electric force is more dominant when the voltage is under 110 V, whereas the elastic force is more dominant when the voltage exceeds 110 V. The curve in Fig. 3(a) is similar to that in fig. 4.1.2 in Chandrasekhar (1992) [36]. We conclude that the pitch of the CLC droplets in a PDCLC film is less than the wavelength of the experiment.

The transparency of a PDLC film is determined by the refractive index of the polymer (n_{p}) and of LC droplets (n_{o}). The refractive index of LC droplets can be changed significantly by applying a substantially lower voltage. A PDLC film is most transparent when the

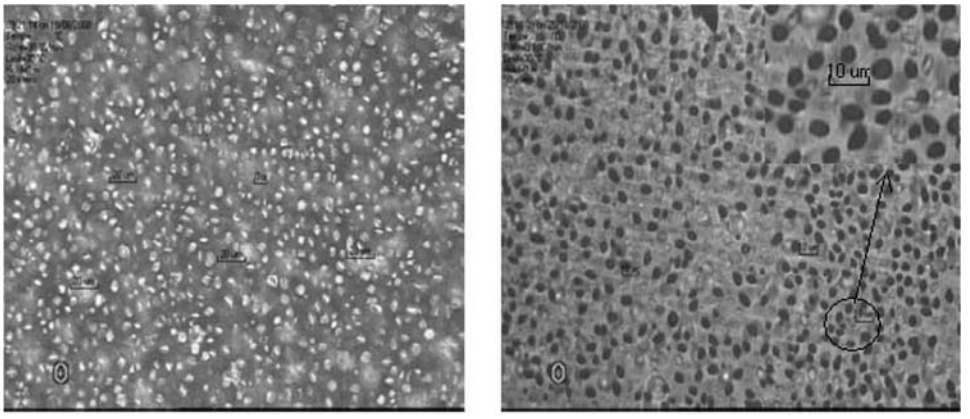

Figure 4. POM micrographs of PDCLC film showing dispersion of CLC droplets in polymer matrix: (a) with polarized light (×500), (b) with unpolarized light (×500).

refractive indices of the polymer and the LC droplets are equal ($n_p = n_o$). The director field of LC droplets is realigned along the direction of the applied electric field. As shown in Fig. 3(b), the transmittance of the PDCLC film is increased under increasing applied electric voltage. The change in transmittance of the PDCLC film as a function of applied voltage is shown in Fig. 3(b). The transmittance of the PDCLC film increased slowly when the applied voltage was below the threshold voltage $V_{th} = 20$ V. The transmittance increased with the increase in voltage, and dramatically increased when the voltage exceeded V_{th}. The transmittance of the PDCLC film reached its maximum when the voltage was 90 V, and it did not change even when the voltagecontinuously increased. The transmittance decreased with voltage decline, and slightly decreased when the voltage declined to 15 V. Because of the competing electric and elastic torques, the director field did not immediately realign along the electric field direction and showed a hysteresis ring of transmittance, with the voltage rising and falling. The maximum transparency is observed at 90 V. The transparency is controlled by the relation between n_p and n_o, which is determined by the applied electric field. The director field of LC droplets tends to align along the direction of the electric field when the applied electric voltage is increased. The refractive index of LC droplets nears the refractive index of the polymer due to the reorientation of the director field under the effect of applied electric field. From the experiment, it was found that the refractive index of LC droplets was most near to the refractive index of the polymer when the applied voltage was 90 V.

The effect of applied voltage on optical rotation and transmittance is shown in Fig. 3. The maximum optical rotation and transparency are observed at 110 V and 90 V, respectively. Through above analysis, the maximum optical rotation is determined by the longest pitch of cholesteric LC droplets at 110 V. This means that the reorientation of the director field induces the longest pitch of the LC droplets at 110 V. However, the reorientation of the director field induces the refractive index of LC droplets to equal the refractive index of the polymer ($n_p = n_o$) at 90 V. The transmittance did not change with the increase in voltage. The different degrees of reorientation of the director field induce distinct effects on optical rotation and transmittance due to changes in the pitch and refractive index of cholesteric LC droplets, respectively. We conclude that the reorientation of

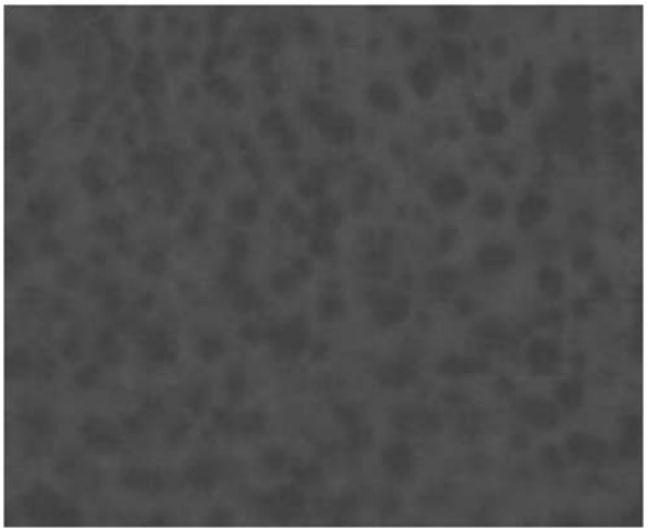

Figure 5. Scanned visible spectrum of PDLC film.

the director field induces different effects on optical rotation and transmittance at different voltages. Thus, the results shown in Figs. 3(a) and (b) are inconsistent.

3.2. Morphology of PDCLC Film by POM

The morphology of the dispersed LC droplets depends on a number of factors, such as the materials used for forming the film, their composition, and, in particular, the film formation process. In the polymerization-induced phase separation performed in this study, the trifunctional monomer and the CLC chosen were miscible with each other, forming an initial homogeneous solution. However, the miscibility of the CLC reduced on exposure to UV. As the polymer network grew, phase separation in alternating polymer-rich and CLC-rich domains occurred. The rapid polymerization of the trifunctional monomer did not allow enough time for the CLC droplets to coalesce. Thus, the CLC droplets did not grow to larger sizes. To form micron-sized CLC droplets, we can accelerate the speed of polymerization by increasing the quantity of the functional group in the photosensitive monomer. POM micrographs of the PDCLC film showing dispersion of CLC droplets in the polymer matrix are shown in Fig. 4.

The CLC droplets have fingerprint texture at room temperature, as shown in Fig. 4(a). The LC droplets developed fingerprint texture under the twist force of chiral agent S-811 during cooling. The rapid polymerization of the photosensitive monomer forced the cholesteric LC droplets out of the polymer matrix, and so, the cholesteric LC droplets did not have enough time to grow into larger droplets. In the end, a PDCLC film was obtained, with uniform, micron-sized chiral fingerprint droplets dispersed in the polymer matrix. The cholesteric LC droplets were etched by methanol for 24 h, as shown in Fig. 4(b), wherein the gray bubbles represent the non-etched cholesteric LC droplets in the polymer matrix. The scales for the cholesteric LC droplets are depicted in Figs. 4(a) and (b). The inset in Fig. 4(b) is an enlarged domain to distinctly depict the size of LC droplets. We concluded that the size of LC droplets was close to 5 μm.

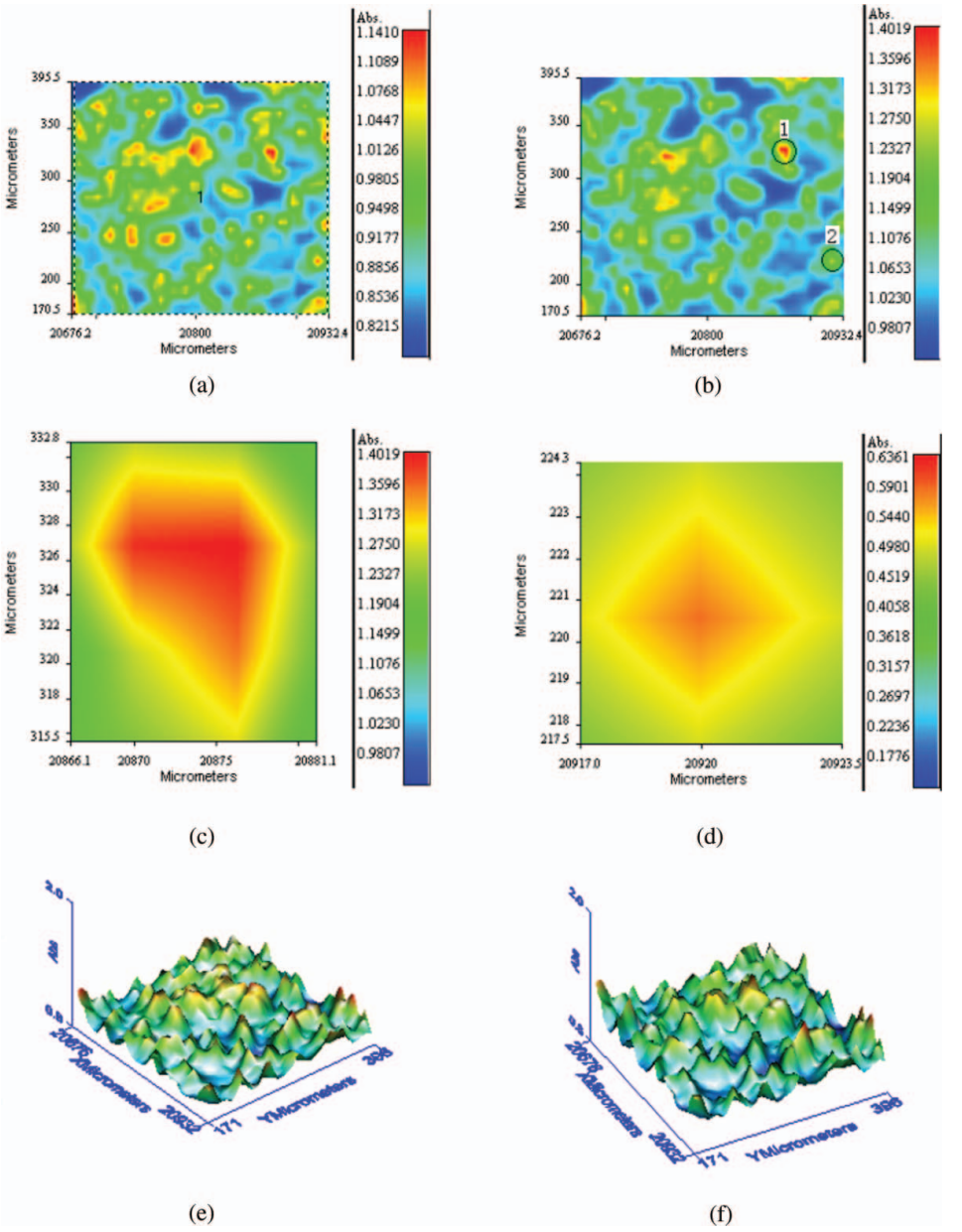

Figure 6. 2D/3D-FTIR adsorption spectrum showing dispersion and size of PDCLC film: (a) total adsorption 2D-FTIR spectrum, (b) single-wavenumber 2D-FTIR spectrum (showing liquid crystal droplets (1) and (2)), (c) enlarged two coalesced liquid crystal droplets (1), (d) enlarged single liquid crystal droplet (2), (e) total adsorption 3D-FTIR spectrum, (f) single-wavenumber 3D-FTIR spectrum.

3.3. Morphology of PDCLC Film by 2D/3D-FTIR

The different groups of complex molecules can be characterized by an FTIR spectrum. A 2D/3D-FTIR spectrum is used for describing the dispersion of a component according

to its characteristic absorption peak in the sample. In this paper, the dispersion of LC droplets in a PDCLC film was described by the 2D/3D-FTIR spectrum. The CLC droplets were characterized by the absorbable wavenumber of the $-C\equiv N$ group, which was set at 2238 cm^{-1}. The equipment used was an FTIR spectrometer (PerKinElmer, Germany) with spectrum spotlight FTIR imaging system (PerKinElmer, Germany), which was pumped by liquid nitrogen. The step of the scanning was set at 6.25 μm. The scanned visible spectrum and 2D/3D-FTIR spectrum obtained by the equipment are shown in Figs 5 and 6, respectively.

The visible spectrum was scanned for selecting a perfect domain to obtain a 2D/3D IR spectrum. As shown in Fig. 5, the black and the grayest domains were LC droplets and the polymer matrix, respectively, and the dispersion of LC droplets was characterized by the visible spectrum. The total absorption 2D-FTIR spectrum is shown in Fig. 6(a). The red and blue colors in the scanned domain represent areas with maximum and minimum intensity of IR absorption, respectively. The yellow color represents the LC droplets in the polymer matrix. The total absorption 3D-FTIR spectrum is shown in Fig. 6(e). The different intensities of absorption are shown as different peak heights in the spectrum. The 2D/3D-FTIR spectra not only described the dispersion of LC droplets but also assessed their size. The single-wavenumber spectrum was derived from the total absorption 2D/3D-FTIR spectrum and the wavenumber was set at 2238 cm^{-1}, which represented the characteristic absorption peak of LC, as shown in Fig. 6(b). The red and blue colors in the PDCLC film represent the areas with maximum and minimum intensity of LC absorption, respectively. The domain of two coalesced LC droplets is marked with a black circinal sign [(1) and (2) in Fig. 6(b)]. Figure 6(c) shows an enlarged version of this domain, and the area measured was 15 μm $\times$ 15 μm. A smaller and a larger LC droplet coalesced at their respective centers to form this domain, and the area of the two LC droplets measured was 7.5 μm $\times$ 6.4 μm and 15 μm $\times$ 9 μm, respectively. The single LC droplet domain is marked as a black circinal sign (2) in Fig. 6(d). Figure 6(d) shows an enlarged version of this domain, and the area measured was 4 μm $\times$ 6 μm. The diameter of the LC droplet measured by the 2D/3D-FTIR spectrum was consistent with the results obtained by POM (determined to be 5 μm). A single-wavenumber 3D-FTIR spectrum depicting dispersion of LC droplets is shown in Fig. 6(f). From the experiment, we concluded that 2D/3D-FTIR spectroscopy is an effective method to study the morphology of LC droplets in PDLC films.

4. Conclusions

In this paper, micron-sized LC droplets were fabricated by rapid polymerization of the selected trifunctional pre-polymer. The effect of applied voltage on optical rotation and transmittance of a PDCLC film were measured by a polarimeter, and discussed by the free-energy minimization process, which resulted from the realignment of the director field under the applied electric field. The morphology of the PDCLC film was studied by POM and a 2D/3D-FTIR spectrum. The size of LC droplets was estimated by the 2D/3D-FTIR spectrum, and was consistent with the results obtained by POM.

In conclusion, we have demonstrated that a PDCLC film with micron-sized CLC domains is suitable for obtaining good optical rotation and transmittance with change in the applied voltage. The dispersion and size of LC droplets were commendably characterized by the 2D/3D-FTIR spectrum. We concluded that 2D/3D-FTIR spectroscopy is a good method to study the morphology of LC droplets in PDLC films.

Acknowledgment

The authors are grateful to the Natural National Science Foundation of China, China's Hi-Tech Research and Development Program (863 Program), and the Commission of Science, Technology and Industry for National Defense (grant no. DBDX2008038) of China.

References

[1] Craighead, H. G., Cheng, J., & Hackwood, S. (1982). *Appl. Phys. Lett.*, *40*, 22.
[2] Doane, J. W., Vaz, N. A., Wu, B. G., & Zumer, S. (1986). *Appl. Phys. Lett.*, *48*, 269.
[3] Smith, G. W., & Vaz, N. A. (1988). *Liq. Cryst.*, *3*, 543.
[4] Drzaic, P. S. (1988). *Liq. Cryst.*, *3*, 1543.
[5] Herod, T. E., & Duran, R. S. (1998). *Langmuir*, *14*, 6956.
[6] Choi, C. H., Kim, B. K., & Kajiyama, T. (1994). *Mol. Cryst. Liq. Cryst.*, *247*, 303.
[7] Nastał, E., Żurańska, E., & Mucha, M. (1999). *J. Appl. Polym. Sci.*, *71*, 455.
[8] Chin, W. K., Hsin, L. P., Lu, H. L., & Shau, M. D. (2000). *J. Polym. Sci. Part B: Polym. Phys.*, *38*, 033.
[9] Zhou, J., Petti, L., Mormile, P., & Roviello, A. (2004). *Opt. Commun.*, *231*, 263.
[10] Petti, L., Mormile, P., & Blau, W. (2003). *J. Opt. Laser Eng.*, *39*, 369.
[11] Petti, L., Mormile, P., Ren, Y., Abbate, M., Musto, P., Ragosto, G., & Blau, W. (2001). *J. Liq. Cryst.*, *28*, 1831.
[12] Yang, D., Lin, J., Li, T., Lin, S., & Tian, X. (2004). *Eur. Polym. J.*, *40*, 1823.
[13] Smith, G. W. (1993). *Mol. Cryst. Liq. Cryst.*, *225*, 113.
[14] Doane, J. W., Golemme, A., West, J. L., Whitehead, J. B., Jr., & Wu, B. G. (1988). *Mol. Cryst. Liq. Cryst.*, *165*, 511.
[15] Sumana, G., & Raina, K. K. (2002). *J. Polym. Mater.*, *19*, 281.
[16] Karapinar, R., O'Neill, M., & Hird, M. (2002). *J. Phys. D: Appl. Phys.*, *35*, 900.
[17] Ryu, J. H., Choi, Y. H., & Suh, K. D. (2006). *Colloids Surf. A: Physicochem. Eng. Aspects*, *275*, 126.
[18] Maschke, U., Coqueret, X., & Benmouna, M. (2002). *Macromol. Rapid Commun.*, *23*, 159.
[19] Huai, Y., Hirotsugu, K., & Kajiyama, T. (2002). *Mol. Cryst. Liq. Cryst.*, *381*, 85.
[20] Karapinar, R. (1998). *J. Phys.*, *22*, 227.
[21] Kitzerow, H. S., & Crooker, P. P. (1991). *Ferroelectrics*, *122*, 183.
[22] Jain, S. C., & Rout, D. K. (1991). *J. Appl. Phys.*, *70*, 6988.
[23] Yang, D. K., Chien, L. C., & Doane, J. W. (1992). *Appl. Phys. Lett.*, *60*, 3102.
[24] Nwabunma, D., Chiu, H.-W., & Kyu, T. (2000). *Macromolecules*, *33*, 1416.
[25] Hoppe, C. E., Galante, M. J., Oyanguren, P. A., & Williams, R. J. (2003). *J. Macromol. Chem. Phys.*, *204*, 928.
[26] Kihara, H., Kishi, R., Miura, T., Kato, T., & Ichijo, H. (2001). *Polymer*, *42*, 1177.
[27] Kihara, H., Miura, T., Kishi, H., & Kaito, A. (2004). *Polymer*, *45*, 6357.
[28] Nakazawa, H., Fujinami, S., Motoyama, M., Ohta, T., Araki, T., Tanaka, H., Fujisawa, T., Nakada, H., Hayashi, M., & Aizawa, M. (2001). *Comput. Theor. Polym. Sci.*, *11*, 445.
[29] Kajiyama, T., Miyamoto, A., Kikuchi, H., & Morimura, Y. (1989). *Chem. Lett.*, *1989*, 813.
[30] Miyamoto, A., Kikuchi, H., Kobayashi, S., Morimura, Y., & Kajiyama, T. (1990). *New Polym. Mater.*, *2*, 27.
[31] Miyamoto, A., Kikuchi, H., Kobayashi, S., Morimura, Y., & Kajiyama, T. (1991). *Macromolecules*, *24*, 3915.
[32] Reamey, R. H., & Montiya, W. (1992). *Proc. SPIE*, *2*, 1665.
[33] Doane, J. W. (1990). Polymer dispersed liquid crystal displays. In: B. Bahadur (Ed.), *Liquid Crystals: Applications and Uses* (Vol. 1), World Scientific: Singapore, p. 361.

[34] Drazaic, P. S. (1988). *Liq. Cryst.*, *3*, 1543.
[35] Meyer, R. B. (1968). *Appl. Phys. Lett.*, *14*, 208; de Gennes, P. G. (1968). *Solid State Commun., 6*, 163.
[36] Chandrasekhar, S. (1992). *Liquid Crystal* (2nd ed.), Press Syndicate of the University of Cambridge: New York.